Bull Earthquake Eng (2015) 13:2893–2914
DOI 10.1007/s10518-015-9744-z

ORIGINAL RESEARCH PAPER

The ductility-based strength reduction factor for the mainshock–aftershock sequence-type ground motions

Chang-Hai Zhai[1,2] · Wei-Ping Wen[1,2] · Shuang Li[1,2] · Li-Li Xie[1,3]

Received: 4 June 2014 / Accepted: 9 March 2015 / Published online: 22 March 2015

Abstract This manuscript investigates the strength reduction factor of single degree of freedom system with constant ductility performance subjected to the mainshock–aftershock sequence-type ground motions. The recorded and artificial sequence-type ground motions are used. The aftershock ground motions in sequence are scaled to have different relative intensity levels. Four hysteretic models are used to simulate the different type of structures. The effects of period, ductility factor, site condition, aftershock, hysteretic behavior and damping are studied statistically. The results indicate that the strong aftershock ground motion has more obvious influences on strength reduction factors in short period region than on those in long period region. The degrading behavior would decrease the strength reduction factor of structure with short period at a magnitude of <20 %, while it would increase that of structure with medium-long period at a maximum level of 20 %. Finally, a predictive model, incorporating the effect of aftershock, is proposed to determine the strength reduction factor in the seismic design.

Keywords Strength reduction factor · Mainshock–aftershock sequence-type ground motion · Relative intensity · Site condition · Hysteretic behavior

1 Introduction

The strong mainshock always triggers lots of aftershocks clustered both in time and space, forming mainshock–aftershock sequence-type ground motions. In the post-mainshock environment, it is impossible to repair the damaged structures before the occurrence of

✉ Chang-Hai Zhai
zch-hit@hit.edu.cn

[1] School of Civil Engineering, Harbin Institute of Technology, Harbin 150090, China

[2] Key Lab of Structures Dynamic Behavior and Control (Harbin Institute of Technology), Ministry of Education, Harbin 150090, China

[3] Institute of Engineering Mechanics, China Earthquake Administration, Harbin 150080, China

subsequent aftershocks due to the short intervals of time. The post-earthquake field reconnaissance (Elnashai et al. 2009; Augenti and Parisi 2010; Ceci et al. 2010; Jing et al. 2011) has confirmed that the strong aftershocks have the potential to increase the damage levels of the structures for the additional damage. Nonetheless, to the authors' best knowledge, all the seismic design codes in the world are based on the single 'design earthquake' without taking into account the danger of aftershock.

Recently, many investigations have been accomplished to examine the influence of aftershock on the damage of structures. Some researchers (Sunasaka et al. 2002; Amadio et al. 2003; Das et al. 2007; Hatzigeorgiou and Beskos 2009; Hatzigeorgiou 2010a, b, c; Goda and Taylor 2012; Goda 2012; Di Sarno 2013; Zhai et al. 2013a, 2014) focused on the inelastic response spectra, such as inelastic displacement ratio, ductility demand, behavior factor and damage spectra for mainshock–aftershock sequence-type ground motions. In addition, several investigations (Fragiacomo et al. 2004; Lee and Foutch 2004; Li and Ellingwood 2007; Hatzigeorgiou and Liolios 2010; Moustafa and Takewaki 2010; Ruiz-García and Negrete-Manriquez 2011; Ruiz-García 2012; Ruiz-García et al. 2012, 2014; Faisal et al. 2013; Zhang et al. 2013; Efraimiadou et al. 2013; Han et al. 2014) have been conducted to study the effects of aftershock on multiple-degree-of-freedom structures.

In the modern seismic codes (CEN 2003; International Building Code (IBC) 2006), the structures are allowed to experience the damage under the moderate to severe earthquakes. The strength reduction factor R is widely used to determine the static seismic force from the elastic design acceleration spectra. The ductility-based strength reduction factor R_μ is an important part in the definition of R by the seismic codes. Lots of researchers (Veletsos and Newmark 1960; Newmark and Hall 1969; Riddell and Newmark 1979a; Miranda 1993; Miranda and Bertero 1994; Miranda and Ruiz-García 2002b; Riddell et al. 2002; Chakraborti and Gupta 2005; Karakostas et al. 2007; Gillie et al. 2010; Qu et al. 2011; Palermo et al. 2013) have investigated the characteristics of R_μ and proposed the corresponding simplified expressions as the design tool. In the all above investigations, just the investigations (Amadio et al. 2003; Hatzigeorgiou 2010a, c) focused on the influence of aftershock or multiple earthquakes on the R_μ. Amadio et al. (2003) repeated the same ground motion two or three times to simulate the sequence-type ground motions. However, as pointed out in other researches (Ruiz-García and Negrete-Manriquez 2011; Zhai et al. 2013a), the sequence-type ground motions generated by this way is unrealistic because the identical ground motion is unlikely to occur two times on the same site. Hatzigeorgiou (2010a, c) studied the R_μ for multiple far-fault and near-fault ground motions with bilinear system. No structural degrading behavior, such as stiffness degrading, strength degrading or pinching behavior, are considered. In addition, the results in investigations (Ruiz-García et al. 2012; Zhai et al. 2014) indicated that the relative intensity of the aftershock ground motion has the significant effect on the seismic performance of structure. However, the current investigations do not specially focus on the influence of relative intensity of the aftershock ground motion on the R_μ.

Based on the above discussions, this manuscript studies the strength reduction factor R_μ with four hysteretic models and lots of mainshock–aftershock sequence-type ground motions. The aftershock ground motions are scaled to have the different intensity levels relative to the mainshock ground motion. The effects of period, ductility factor, site condition, aftershock, hysteretic behavior and damping ratio on the R_μ are studied statistically. Finally, a predictive model is proposed to facilitate the application of R_μ in the seismic design.

2 Strength reduction factors

In this manuscript, the strength reduction factor is defined as the ratio of strength demand of elastic structure for the mainshock ground motion to the yield strength of corresponding inelastic structure for the certain ductility level and sequence-type ground motion. Mathematically it can be expressed as:

$$R_{\mu} = \frac{F_{\mathrm{e,ms}}}{F_{\mathrm{y}}} \tag{1}$$

where $F_{\mathrm{e,ms}}$ = strength demand on an infinitely elastic SDOF system during the prescribed mainshock ground motion, F_{y} = yield strength of the corresponding inelastic SDOF system, making the system satisfy the criterion of ductility level under the mainshock–aftershock sequence-type ground motions.

The ductility factor is defined as:

$$\mu = \frac{x_{\mathrm{m}}}{x_{\mathrm{y}}} \tag{2}$$

where x_{m} = maximum displacement demand of inelastic structure under the ground motion, x_{y} = yield displacement of inelastic structure.

The following four hysteretic models, which have been used in the references (Zhai et al. 2013b, 2014; Wen et al. 2014), are used to investigate the effect of hysteretic behavior on the R_{μ}: (1) Elastic–Perfectly-Plastic (EPP) model, representing the non-degrading systems; (2) Modified Clough (MC) model, simulating the flexural behavior that exhibit stiffness degradation at reloading; (3) Pinching model, simulating the reinforced concrete structures with crack opening and closure, or the steel structures with connection slip behavior; (4) Stiffness Strength Degradation (SSD) model based on the three parameter model, representing global behavior of systems exhibiting stiffness degradation and strength deterioration during reloading branches.

Riddell and Newmark (1979b) pointed out that several deficiencies exist in the original Clough model, resulting from the lack of constitutive rules for treating incomplete and small amplitude loops. These deficiencies can cause unrealistic seismic responses, such as releasing energy instead of dissipating energy under some unloading–reloading circumstances. Thus the modified Clough model was proposed by the past researches (Mahin and Bertero 1975, 1976; Riddell and Newmark 1979b) to avoid the above deficiencies, and this model is extensively used to study the structural response (Miranda and Ruiz-García 2002a, b; Iervolino et al. 2006; Tong and Zhao 2007). The pinching model used here was developed by Rahnama and Krawinkler (1993). The detailed hysteretic rules of this model were introduced and described in the literature (Rahnama and Krawinkler 1993). The stiffness strength degradation model is based on the three parameter model (Kunnath et al. 1990; Valles et al. 1996), which was calibrated with the experimental results by Valles et al. (1996) and was included in the software IDARC.

The inelastic SDOF systems with a set of 60 periods between 0.1 and 6.0 s with an interval of 0.1 s are considered in this manuscript. The viscous damping ratio is assumed to be 5 %. Five ductility factors μ = 2, 3, 4, 5 and 6 are selected to consider the different ductility performances. Figure 1 shows the flowchart for the computation of the ductility-based strength reduction factor for the mainshock–aftershock sequence-type ground motion. The strength reduction factor R_{μ} is calculated by gradually reducing the applied

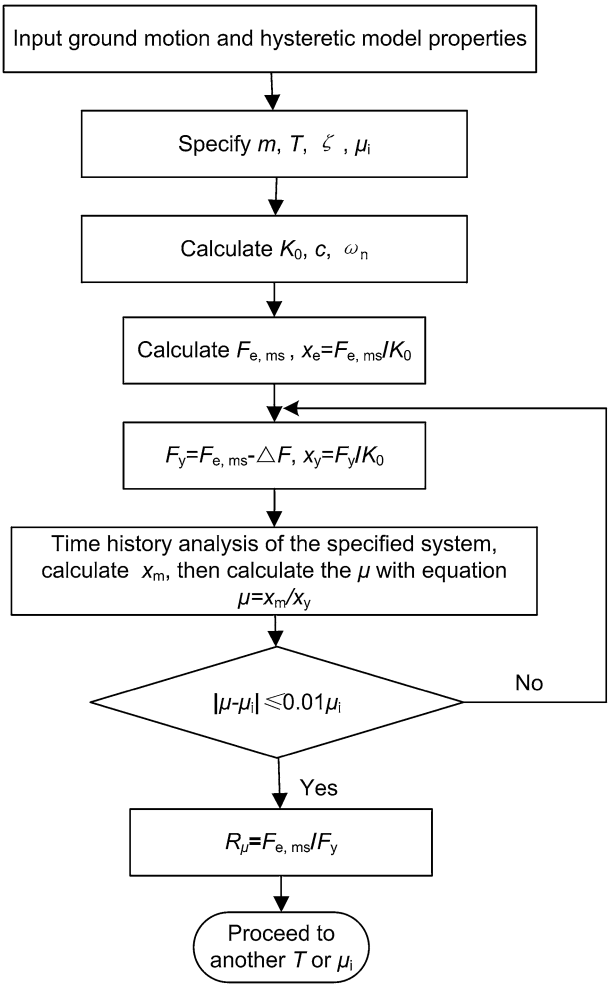

Fig. 1 The flowchart for the computation of the ductility-based strength reduction factor for the mainshock–aftershock sequence-type ground motion

strength of SDOF system from the corresponding elastic strength demand $F_{e,ms}$ until the specified μ is achieved within a tolerance (1 % is used in this manuscript).

In this manuscript, the in-house codes are developed with Fortran language to simulate the different hysteretic models. Then these in-house codes are used to compute the response of SDOF system under the mainshock–aftershock sequence-type ground motions.

3 Ground motions

When constructing the mainshock–aftershock sequence-type ground motions, several researchers (Ruiz-García and Negrete-Manriquez 2011; Goda and Taylor 2012; Zhang et al. 2013) selected all the available aftershock ground motions (satisfying their own criterions)

in the sequence-type ground motion. The problem of this method is that, in the final selected database, many sequence-type ground motions (possess a big part in the database) include only one aftershock ground motion, while others contain multiple aftershock ground motions. The statistical results of these sequence-type ground motions would mix the effect of one aftershock on the seismic response of structure with that of multiple aftershocks. In this case, many investigations (Lee and Foutch 2004; Li and Ellingwood 2007; Ruiz-García et al. 2012, 2014; Han et al. 2014) just select one aftershock ground motion in the sequence-type ground motions. The results in these investigations also indicated that these sequence-type ground motions can provide valuable information about the influence of aftershock on the seismic response of structure. Thus, in this manuscript, just one aftershock ground motion is selected in the sequence-type ground motion.

In this manuscript, the recorded mainshock–aftershock sequence-type ground motions are selected from the Pacific Earthquake Engineering Research Center (PEER) Next Generation Attenuation (NGA) relationships database (http://peer.berkeley.edu/nga/). For the seismic sequence recorded on a given station, if the mainshock ground motion and one of aftershock ground motions both satisfy the characteristics specified in this manuscript, the mainshock ground motion and this aftershock ground motion will be used to generate a sequence-type ground motion. The specified characteristics of the ground motions are: (1) recorded on accelerographic stations where enough information about the geological and geotechnical conditions at the site is available; (2) recorded on free field stations or on the ground level of the structures; (3) the peak ground acceleration (*PGA*) of mainshock ground motion and aftershock ground motions is >0.1 g, respectively. Finally, a total of 218 mainshock–aftershock sequence-type ground motions are obtained with this approach. Table 1 shows the information of the mainshock–aftershock sequences used in this paper and the number of ground motions in each seismic sequence.

It should be pointed out that all the above 218 sequence-type ground motions are recorded on the site classes B and C, according to the site classification method of United States Geological Survey (USGS). In order to supplement the sequence-type ground motions on site classes A and D, the artificial mainshock–aftershock sequence-type ground motions are used in this manuscript. The details of the generating method are introduced in the following paragraphs.

For the given site class (site class A or D), a group of recorded ground motions with *PGA* being larger than 0.1 g are selected as seed ground motions from the PEER–NGA

Table 1 Information of the mainshock–aftershock sequences used in this paper and the number of ground motions in each seismic sequence

Earthquake name	Mainshock		Aftershock		Number of ground motions
	Time	M_W	Time	M_W	
Imperial Valley	1979-10-15, 23:16	6.53	1979-10-15, 23:19	5.01	19
Northridge	1994-01-17, 12:31	6.69	1994-01-17, 12:32	6.05	9
			1994-03-20, 21:20	5.28	32
ChiChi	1999-09-20	7.62	1999-09-20, 17:57	5.9	10
			1999-09-20, 18:03	6.2	40
			1999-09-20, 21:46	6.2	21
			1999-09-22, 00:14	6.2	42
			1999-09-25, 23:52	6.3	45

database. Then the artificial sequence-type ground motions are generated by randomly combining two different seed ground motions. It is known that the interdependence exists between mainshock and aftershock ground motions, and the real sequence-type ground motions can reflect this interdependence perfectly. However, there is no enough valuable information (e.g. ground motion parameters relationship between mainshock and aftershock) to quantitatively and clearly describe this interdependence. This randomly combining method has been applied in several researches (Hatzigeorgiou 2010a, b; Faisal et al. 2013; Zhai et al. 2013a; Ruiz-García et al. 2014). Though the artificial sequence-type ground motions may not perfectly reflect this interdependence and errors may be induced by using these artificial sequence-type ground motions to compute the structural response, the results in these investigations still showed that the artificial sequence-type ground motions generated by this method have the acceptable potential to study the influence of multiple successive ground motions on the seismic response of structures. Thus this randomly combining method is also used in this manuscript.

Table 2 summarizes the information of the single ground motions used to generating the sequence-type ground motions on site classes A and D. Table 3 presents the number of recorded and artificial sequence-type ground motions on different site classes.

The relative peak ground acceleration of aftershock ground motion ∇PGA is defined as:

$$\nabla PGA = \frac{PGA_{\mathrm{as}}}{PGA_{\mathrm{ms}}} \tag{3}$$

where PGA_{as} is the peak ground acceleration of aftershock ground motion, PGA_{ms} is the peak ground acceleration of mainshock ground motion.

Table 2 The information of seed ground motions for simulating the mainshock–aftershock sequence-type ground motions on site class A and D

Earthquake	Time	Magnitude M_{W}	Number of ground motions	
			Site class A	Site class D
Seed ground motions				
San Fernando	1971-02-09, 14:00	6.61	3	0
Irpinia	1980-11-23, 19:34	6.9	4	0
Whittier Narrows	1987-10-01, 14:42	5.99	6	2
Loma Prieta	1989-10-18	6.93	4	10
Kocaeli	1999-08-17	7.51	4	2
ChiChi	1999-09-20	7.6	2	2
Yountville	2000-09-03	5.0	0	2
All	–	–	20	18

Table 3 The number of recorded and artificial sequence-type ground motions on different site classes

Site classes	V_{S30} (m/s)	Number of ground motions	
		Recorded	Artificial
A	>750	0	129
B	360–750	116	0
C	180–360	102	0
D	<180	0	111

The ∇PGA is used to represent the relative intensity level of aftershock ground motion with respect to the mainshock ground motion. In order to study the influence of relative intensity of aftershock ground motion on the strength reduction factor R_μ, the aftershock ground motion is scaled to have four levels of relative intensity (i.e. $\nabla PGA = 0.5, 0.8, 1.0$ and 1.5) for each sequence-type ground motion. It is the fact that the intensity of aftershock ground motion is generally smaller than the mainshock ground motion, due to the lower magnitude of aftershock. But the aftershock ground motions with greater intensity with respect to that of mainshock ground motions do exist in the past seismic sequences (Zhai et al. 2014), though the number of these aftershock ground motions is pretty lower than that of other aftershock ground motions. In order to provide a design tool considering aftershock ground motions with various relative intensities which exist in the past seismic sequences, the value of ∇PGA being 1.5 is used to simulate the extreme case of aftershock ground motion.

4 Statistical analyses

4.1 Mean strength reduction factors

A total of 137,400 strength reduction factors R_μ of EPP systems are computed as part of this investigation, for 458 sequence-type ground motions, 60 periods and 5 ductility factors. Mean R_μ are then computed by averaging results for each period, each ductility factor μ and each site class. It should be noted that the quantification of the different spectral regions can facilitate the analysis and discussion. However, in the realistic case, it is difficult to strictly define the boundary between the different spectral regions. In this manuscript, the short, medium and long period regions are approximately corresponded to (0.0–0.5 s), (0.5–1.5 s) and (1.5–6.0 s). But in some cases, the above definition is not exact and proper to describe the characteristics of the results, and thus the specifically period range is used to analyze the results. Due to the space limitation, just the results of limited cases are presented in the following sections, while other cases having the similar results are not presented.

Figure 2 shows the mean R_μ of EPP system for the four site classes and the sequence-type ground motions with $\nabla PGA = 0.5$. In general, the mean R_μ shows the same general trend regardless of site conditions. In the short period region, mean R_μ is strongly dependent on the period and increases sharply with the increase of period. In the medium-long period region, the influence of period on the mean R_μ is not significant. The mean R_μ in medium-long period region is approximately period independent in comparison with that in short period region. In the long period region, the mean R_μ varies approximately around the corresponding μ when the period increases.

In the whole period region, mean R_μ increases with the increase of μ. In the medium-long period, the ductility factor μ has the significant effect on the R_μ. In the short period region, the influence of μ on R_μ reduces gradually as the period decreases. Take the mean R_μ on site class B as the example, the difference between the mean R_μ of $\mu = 2$ and 4 is about 80 % for the structure with period being 0.5 s, while this difference decreases to 30 % for the structure with period being 0.1 s.

The limiting period dividing the period region whether the mean R_μ is period independent or not depends on the ductility factor μ and site conditions. In general, this limiting period increases as the μ increases. For the R_μ on site class A, the limiting period increases

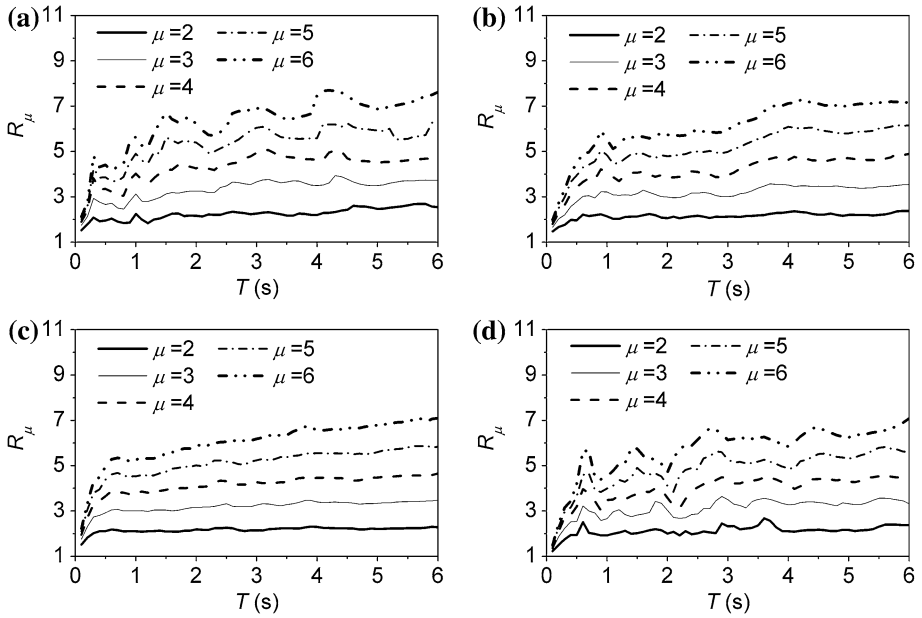

Fig. 2 The mean R_μ of EPP system for the four site classes and the sequence-type ground motions with $\nabla PGA = 0.5$: **a** site class A, **b** site class B, **c** site class C, **d** site class D

from 0.3 to 0.8 s as the μ increase from 2 to 6. For the R_μ of $\mu = 4$, the limiting period increases from 0.5 to 1.2 s as the site class changes from B to D.

It can be noted that the curves in Fig. 2 are smoother for site classes B and C in comparison to the ones that correspond to A and D site classes. This phenomenon may due to the errors induced by using the artificial sequence-type ground motions to compute the structural response, as pointed out in Sect. 3.

It is common to give the general information of strength reduction factors regardless of the site conditions. Figure 3 presents the mean R_μ of EPP system for all sequence-type ground motions with $\nabla PGA = 0.5$. It is obvious that the mean R_μ in Figs. 2 and 3 shows the similar trend with the period and μ. The limiting period increases from 0.3 to 1.0 s as μ increases from 2 to 6.

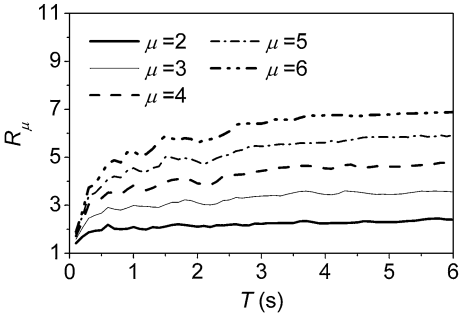

Fig. 3 The mean R_μ of EPP system for all sequence-type ground motions with $\nabla PGA = 0.5$

4.2 Dispersion of strength reduction factors

In this section, the coefficient of variation (COV) is used to evaluate the dispersion of the R_μ. The COV is defined as the ratio of the standard deviation to the mean. Figure 4 illustrates the COVs of R_μ on four site classes for EPP system and sequence-type ground motions with $\nabla PGA = 0.5$.

In the whole period region, COVs do not significantly change with the variation of the period, and thus are approximately period independent. Except a few COVs on site class D, all the COVs in Fig. 4 are smaller than 0.5. In general, COVs of R_μ on different site classes show the similar trend and the differences of COVs on different site classes are small. However, it can be found that COVs are relatively sensitive to the μ and increase with the increase of μ. For example, the COVs are about 20 % for $\mu = 2$ and increase to 40 % approximately for $\mu = 6$, as shown in Fig. 4.

4.3 Effect of site conditions

In order to investigate the influence of site conditions on the R_μ, the mean R_μ on different site classes are normalized by the mean R_μ on all site classes, respectively. In this way, the error produced by ignoring the influence of site conditions when evaluating the R_μ on different site classes can be investigated quantitatively. Figure 5 presents the normalized mean R_μ of EPP system for different site classes and sequence-type ground motions with $\nabla PGA = 0.5$.

It can be seen that the normalized mean R_μ in Fig. 5a can reach 1.2, indicating that the mean R_μ on all site classes would underestimate the mean R_μ on site class A at a maximum

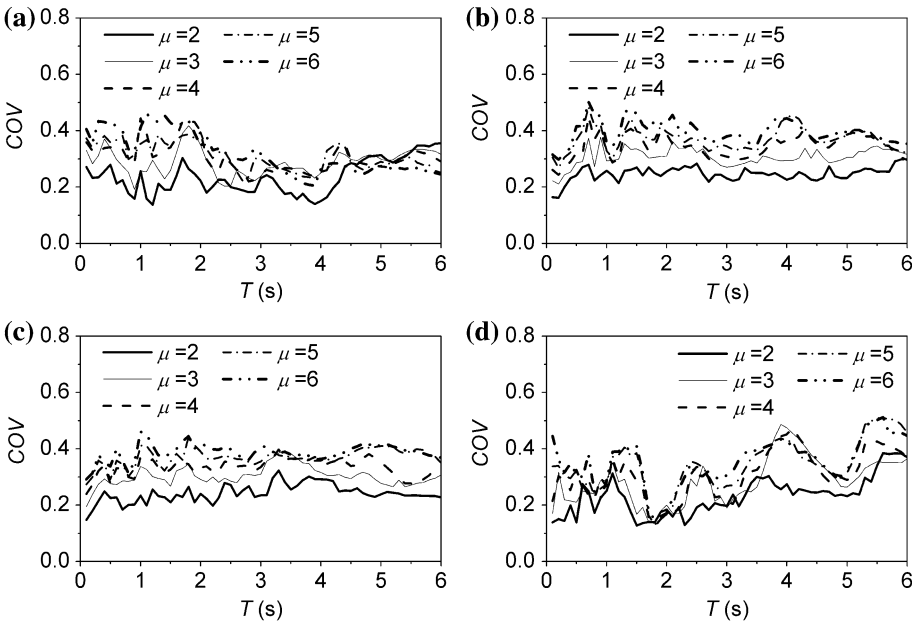

Fig. 4 The COVs of R_μ on four site classes for EPP system and sequence-type ground motions with $\nabla PGA = 0.5$: **a** site class A, **b** site class B, **c** site class C, **d** site class D

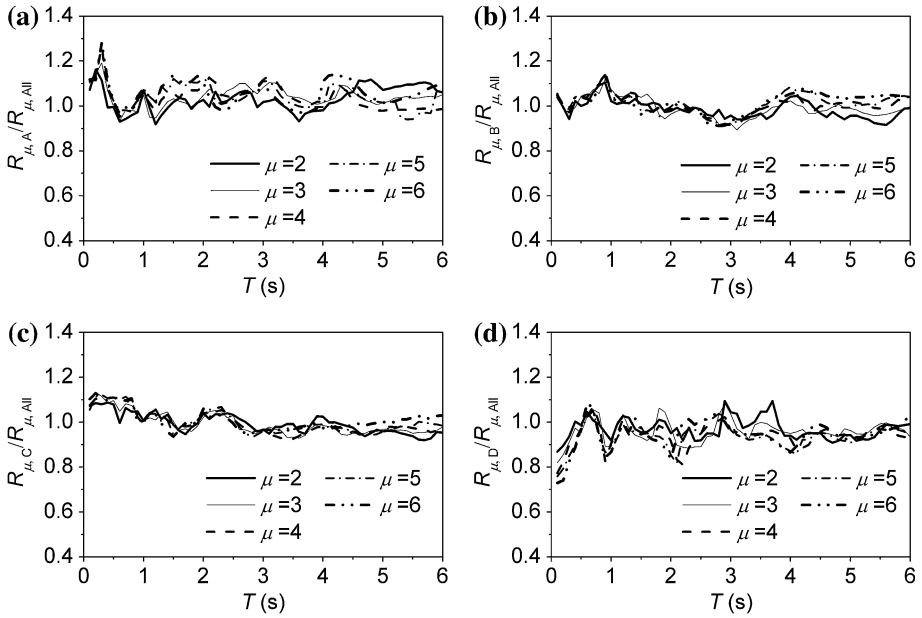

Fig. 5 The normalized mean R_μ of EPP system for different site classes and sequence-type ground motions with $\nabla PGA = 0.5$: **a** site class A, **b** site class B, **c** site class C; **d** site class D

level of 20 %. All the values of normalized mean R_μ in Fig. 5b, c are within the interval [0.9, 1.1]. This phenomenon means that the errors are within 10 % when evaluating the R_μ on site classes B or C with the mean R_μ on all site classes. The normalized mean R_μ in Fig. 5b, c is not clearly dependent on the μ.

In the short period region, the normalized mean R_μ in Fig. 5d is smaller than 1.0 and the minimum value can reach 0.7, meaning that the mean R_μ on all site classes would overestimate the mean R_μ on site class D at a maximum level of 30 %. The normalized mean R_μ in this period region decreases as the μ increases, indicating that the effect of site condition on R_μ of site class D is more obvious for structures with larger inelastic deformation. Thus, for μ smaller than 3 the errors produced by neglecting the influence of site condition are commonly smaller than 20 %, while the corresponding errors can reach 30 % for $\mu = 6$, as can be seen in Fig. 5d.

In the medium-long period region, the normalized mean R_μ in Fig. 5d varies within the interval [0.9, 1.1]. This phenomenon indicates that the difference between the mean R_μ on site class D and the mean R_μ on all site classes is within 10 % for structures with medium-long periods. Similar to the results in Fig. 5a–c, the normalized mean R_μ in this region is also not clearly dependent on the μ.

For the structure with short period, the seismic response on site class A (rock site) is generally smaller than that on other site classes, while the seismic response on site class D (soft soil site) is generally larger than that on other site classes (Zhai et al. 2013a). Thus in the short period region, the mean R_μ on site class A is greater than that on all site classes, while the mean R_μ on site class D is smaller than that on all site classes.

4.4 Effect of aftershock

The effect of aftershock on the R_μ is studied in this section. The ratio between the R_μ of sequence-type ground motion and that of corresponding mainshock ground motion, denoted as $R_{\mu,\text{seq}}/R_{\mu,\text{ms}}$, is computed for each sequence-type ground motion. Then the mean $R_{\mu,\text{seq}}/R_{\mu,\text{ms}}$ of all sequence-type ground motions with constant ∇PGA is computed for each period and each μ.

Figure 6 shows the mean $R_{\mu,\text{seq}}/R_{\mu,\text{ms}}$ for the sequence-type ground motions with $\nabla PGA = 0.5$ and different hysteretic models. It can be seen that all the mean $R_{\mu,\text{seq}}/R_{\mu,\text{ms}}$ values in Fig. 6 are within the interval [0.97, 1.0], indicating that the aftershock ground motion with $\nabla PGA = 0.5$ would decrease the strength reduction factor at a level of <3 %. Thus the effect of aftershock ground motion with$\nabla PGA = 0.5$ on the R_μ can be ignored in the engineering practice.

Figure 7 presents the mean $R_{\mu,\text{seq}}/R_{\mu,\text{ms}}$ for the sequence-type ground motions with $\nabla PGA = 1.0$ and different hysteretic models. For systems with periods >0.5 s, the mean $R_{\mu,\text{seq}}/R_{\mu,\text{ms}}$ varies slightly with the change of period and is approximately period independent. The values of mean $R_{\mu,\text{seq}}/R_{\mu,\text{ms}}$ in the whole period region are generally within the interval [0.9, 0.95], meaning that the aftershock ground motion with $\nabla PGA = 1.0$ would decrease the strength reduction factor R_μ of structure at a level of <10 %.

From the Figs. 6 and 7, it can be seen that the values of mean $R_{\mu,\text{seq}}/R_{\mu,\text{ms}}$ are generally comparable for different hysteretic models. This phenomenon indicates that the aftershock ground motion has similar effects on the R_μ for different hysteretic models.

In order to compare the influences of aftershock ground motions with different relative intensities ∇PGA on the R_μ more clearly, Fig. 8 illustrates mean $R_{\mu,\text{seq}}/R_{\mu,\text{ms}}$ for system with $\mu = 4$ and sequence-type ground motions with different ∇PGA. It is clear that the

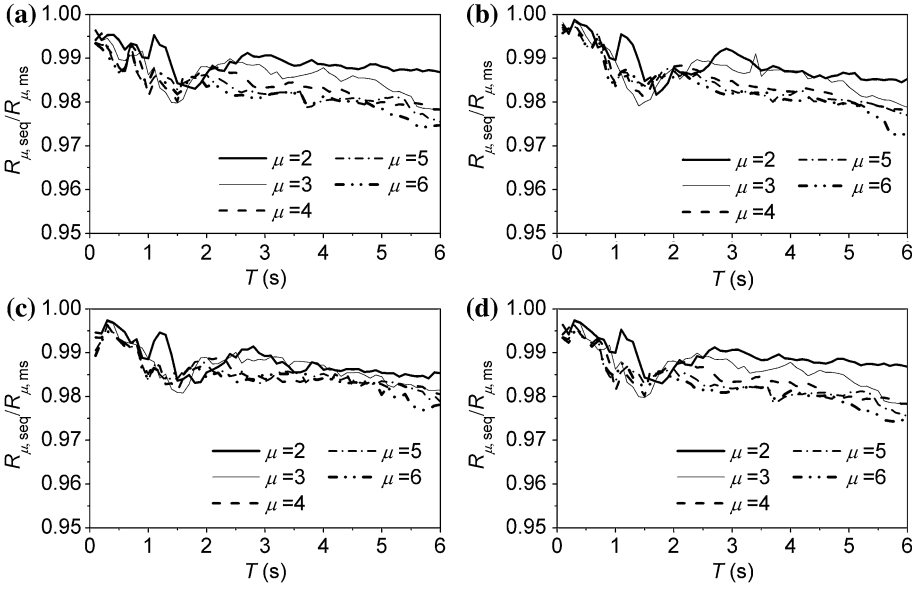

Fig. 6 The mean $R_{\mu,\text{seq}}/R_{\mu,\text{ms}}$ for the sequence-type ground motions with $\nabla PGA = 0.5$ and different hysteretic models: **a** EPP model, **b** MC model, **c** PH model, **d** SSD model

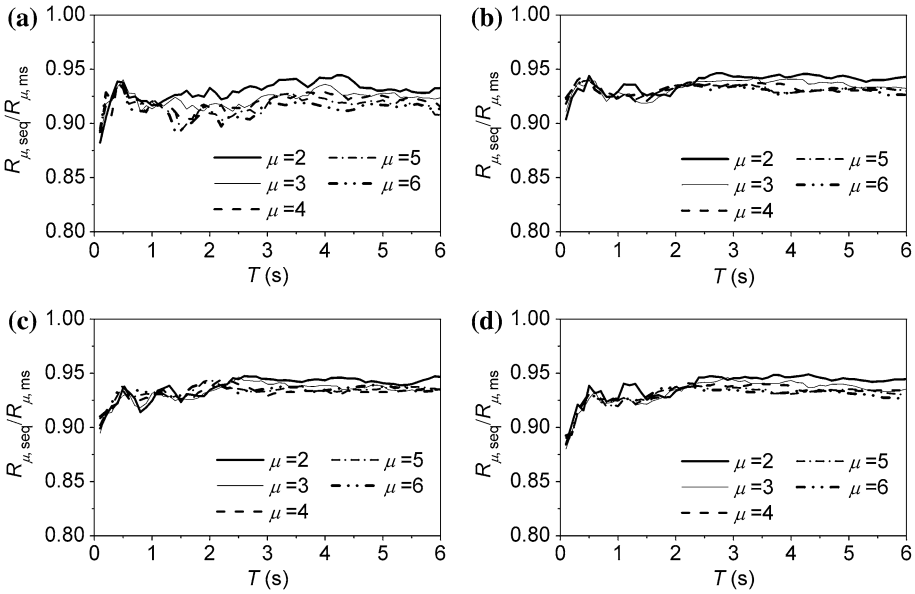

Fig. 7 The mean $R_{\mu,\mathrm{seq}}/R_{\mu,\mathrm{ms}}$ for the sequence-type ground motions with $\nabla PGA = 1.0$ and different hysteretic models: **a** EPP model, **b** MC model, **c** PH model, **d** SSD model

mean $R_{\mu,\mathrm{seq}}/R_{\mu,\mathrm{ms}}$ in Fig. 8 decreases with the increase of ∇PGA. For the mean $R_{\mu,\mathrm{seq}}/R_{\mu,\mathrm{ms}}$ of the sequence-type ground motion with $\nabla PGA = 1.5$, the corresponding values in the short period region can be smaller than 0.8, while the corresponding values in the medium-long period region are always >0.85. These phenomena indicate that the aftershock ground motion with $\nabla PGA = 1.5$ can decrease the R_μ of structure with short period at a level of more than 20 %, while this decrease magnitude is always <15 % for structure with medium-long period. The above results reveal that the effects of aftershock on the mean R_μ are related to the period, ductility factor and intensity of aftershock ground motion.

For the structure which has been damaged by the mainshock, the subsequent aftershocks may induce the additional damage due to the damage accumulation. In order to satisfy the given ductility factor, the structure under the seismic sequence needs greater yield strength in comparison to the structure under the mainshock alone. Moreover, the stronger aftershocks are included in the seismic sequence, the greater yield strength is needed. Thus the aftershock has the potential to reduce the R_μ with respect to the mainshock alone, and the reduction depends on the intensity of the aftershock ground motion, just as revealed by the above results.

Similarly, the effects of aftershock on the dispersion of the R_μ are investigated through the ratios of the COVs of $R_{\mu,\mathrm{seq}}$ to those of the $R_{\mu,\mathrm{ms}}$. Figure 9 shows the $\mathrm{COV}_{\mathrm{seq}}/\mathrm{COV}_{\mathrm{ms}}$ for the sequence-type ground motions with $\nabla PGA = 1.0$ and different hysteretic models. Except the periods smaller than 0.3 s, the ratios in Fig. 9 are generally >1.0, and the maximum ratio exceeds 1.20. This phenomenon indicates that the strong aftershock with the same intensity with that of mainshock may increase the dispersion of the R_μ in a maximum level of 20 %. The ratios of COV in Fig. 9 depend on the ductility factor μ, and this dependence would gradually vanish with the increase of the μ. The COV is the ratio of the mean R_μ to the standard deviation of the R_μ. In comparison with the results for the

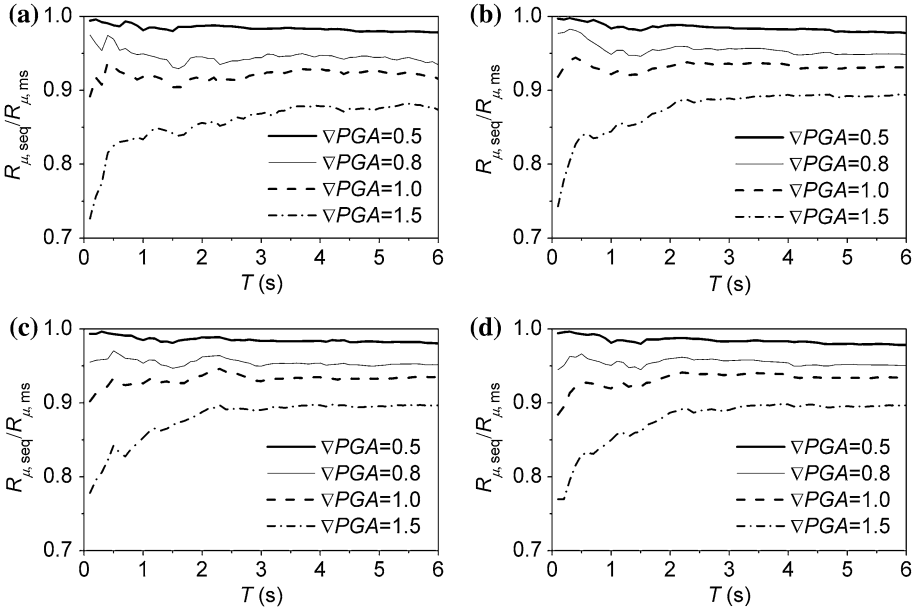

Fig. 8 The mean $R_{\mu,\mathrm{seq}}/R_{\mu,\mathrm{ms}}$ for different hysteretic models with $\mu = 4$ and sequence-type ground motions with different ∇PGA: **a** EPP model, **b** MC model, **c** PH model, **d** SSD model

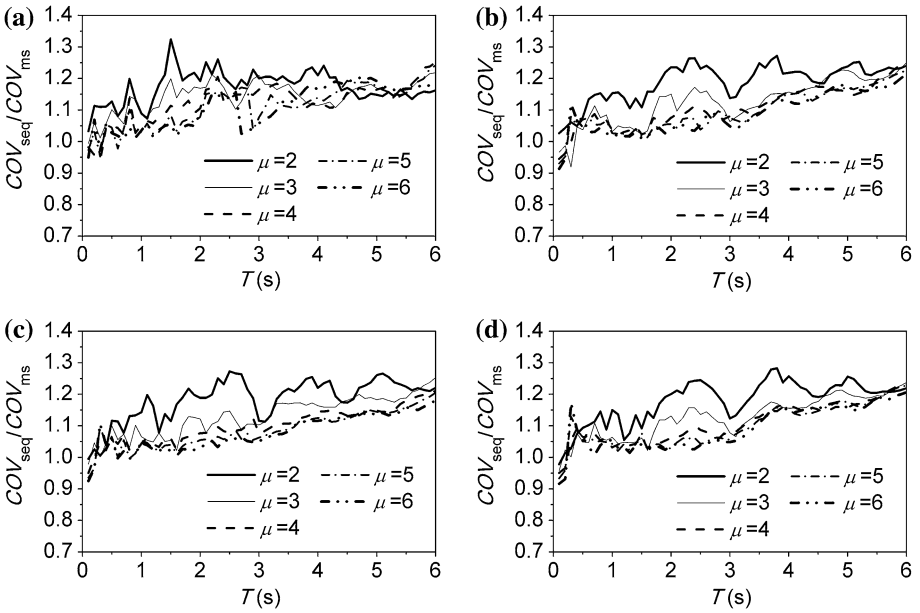

Fig. 9 The mean $COV_{\mathrm{seq}}/COV_{\mathrm{ms}}$ for the sequence-type ground motions with $\nabla PGA = 1.0$ and different hysteretic models: **a** EPP model, **b** MC model, **c** PH model, **d** SSD model

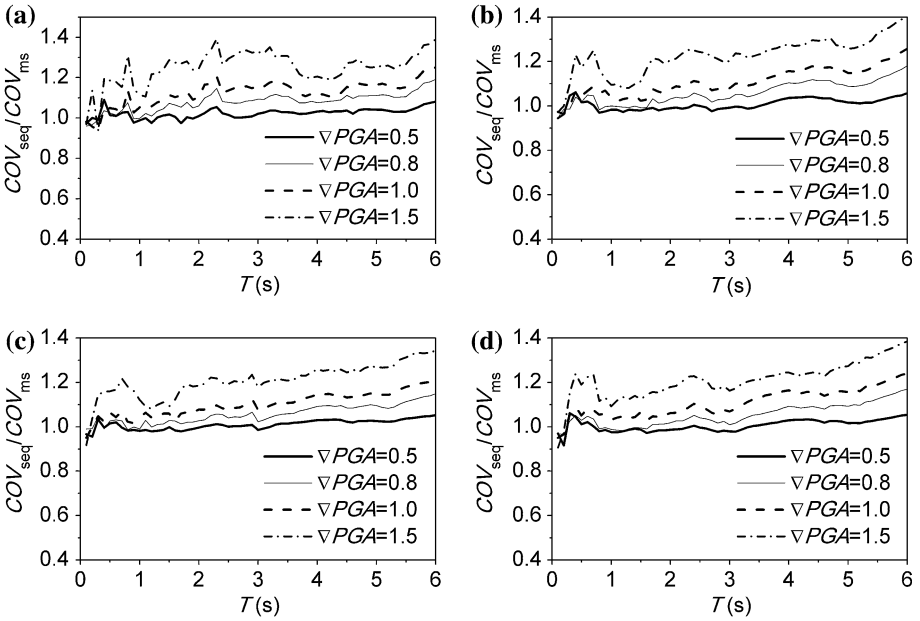

Fig. 10 The mean COV_{seq}/COV_{ms} for different hysteretic models with $\mu = 4$ and sequence-type ground motions with different ∇PGA: **a** EPP model, **b** MC model, **c** PH model, **d** SSD model

mainshock alone, the mean response of structure and the corresponding standard deviation are both enhanced by the strong aftershocks. When the enhancement of the mean response exceeds that of the standard deviation, the aftershock increases the COV of the structural responses. The influences of aftershock on the COV of the R_μ depend on the period, ductility factor and intensity of aftershock ground motion (explained in the next paragraph).

Figure 10 illustrates $\mathrm{COV}_{seq}/\mathrm{COV}_{ms}$ for system with $\mu = 4$ and sequence-type ground motions with different ∇PGA. The ratios correspond to ∇PGA being 0.5 and 0.8 are within the interval [0.9, 1.1], indicating that the influences of aftershock ground motion with ∇PGA smaller than 1.0 are approximately within 10 %. The ratios in Fig. 10 generally increase as the intensity of aftershock ground motion increases. The results in Figs. 8 and 10 show the consistence that the stronger aftershock has more obvious influences.

4.5 Effect of hysteretic behavior

In this section, the influence of degrading behavior on the R_μ is investigated. In this manuscript, the degrading systems are simulated by the MC model, PH model and SSD model. The ratio between the R_μ of the degrading system and that of EPP system, denoted as $R_{\mu,\mathrm{degrading}}/R_{\mu,\mathrm{EPP}}$, is computed for each sequence-type ground motion. Then the mean $R_{\mu,\mathrm{degrading}}/R_{\mu,\mathrm{EPP}}$ of all sequence-type ground motions with constant ∇PGA are calculated for each period and each μ.

Figure 11 shows the mean $R_{\mu,\mathrm{degrading}}/R_{\mu,\mathrm{EPP}}$ for sequence-type ground motions with $\nabla PGA = 0.5$ and different hysteretic models. For the periods being smaller than 1.0 s, the mean $R_{\mu,\mathrm{degrading}}/R_{\mu,\mathrm{EPP}}$ has strong dependence on the period and increases as the period

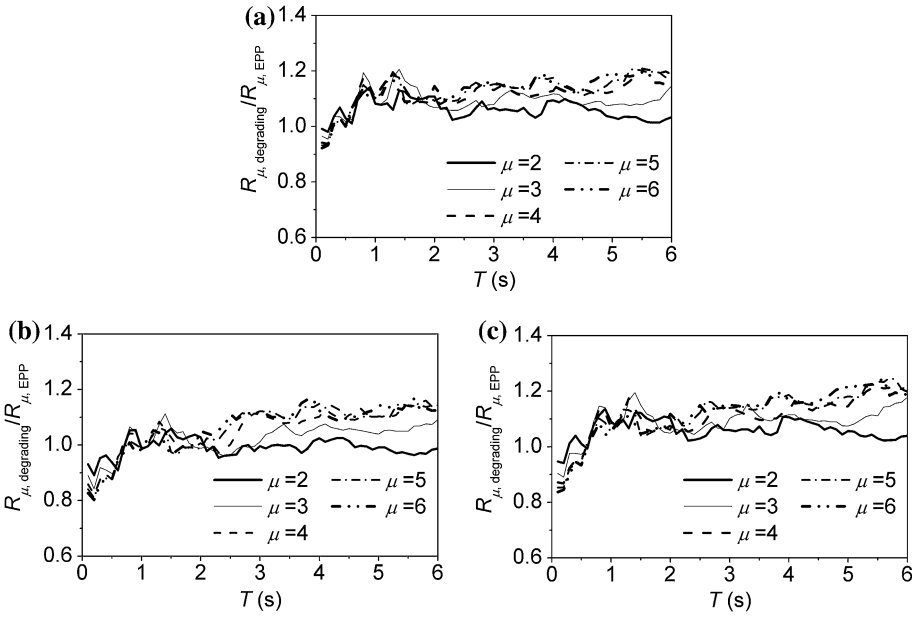

Fig. 11 The mean $R_{\mu,\text{degrading}}/R_{\mu,\text{EPP}}$ for sequence-type ground motions with $\nabla PGA = 0.5$ and different hysteretic models: **a** MC model, **b** PH model, **c** SSD model

increases. When the period is >1.0 s, the mean $R_{\mu,\text{degrading}}/R_{\mu,\text{EPP}}$ region has weaker dependence on the period. When the period is very small (e.g. $T = 0.2$ s), the degrading behavior decreases the R_μ. When the period is beyond the limitation period, the degrading behavior increases the R_μ. This limitation period varies for different degrading models (i.e. 0.3 s for MC model, 0.8 s for PH model and 0.5 s for SSD model).

All the values of mean $R_{\mu,\text{degrading}}/R_{\mu,\text{EPP}}$ in Fig. 11 are generally within the interval [0.8, 1.2]. This phenomenon means that degrading behavior would decrease the R_μ of structure with short period at a magnitude of <20 %, while increase the R_μ of structure with medium-long period as a maximum level of 20 %. For the degrading systems with long periods, the smaller hysteretic loops are more than those of non-degrading systems. For the case of constant μ, the seismic response of degrading system with long periods tends to be smaller than that of non-degrading system. Thus the R_μ factors of degrading system are greater than those of non-degrading system in long period region. These above results and phenomena are consistent with the conclusions stated by past researches (Riddell and Newmark 1979a; Riddell et al. 2002).

4.6 Effect of damping

In order to investigate the influence of damping on the R_μ, the R_μ of EPP system with damping ratio $\zeta = 0.02$ and 0.1 is calculated. Then R_μ of EPP system with $\zeta = 0.02$ and 0.1 is normalized by the R_μ of EPP system with $\zeta = 0.05$ for each sequence-type ground motion. In final, the mean normalized R_μ of all sequence-type ground motions with constant ∇PGA is computed for each period and each μ.

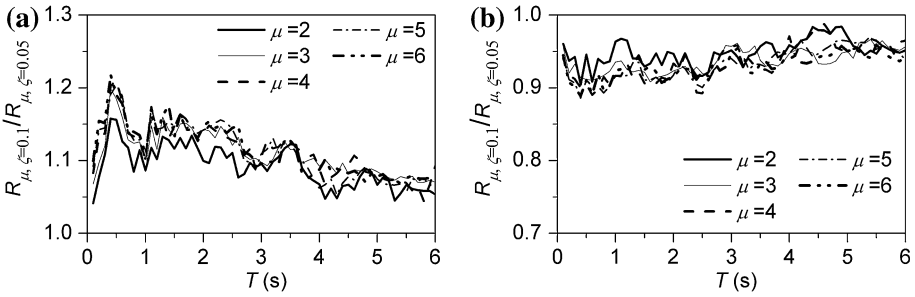

Fig. 12 The mean normalized R_μ of all sequence-type ground motions with $\nabla PGA = 0.5$: **a** $\zeta = 0.02$, **b** $\zeta = 0.1$

Figure 12 presents the mean normalized R_μ of all sequence-type ground motions with $\nabla PGA = 0.5$. It can be seen that the mean normalized R_μ in Fig. 12a is >1.0, while that in Fig. 12b is smaller than 1.0. This phenomenon means that the strength reduction factor R_μ decreases as the damping ratio ζ increases. It is well known that the response of elastic and inelastic structure will be reduced when the structural damping increases. All the input energy of elastic system is dissipated by the structural damping, while just part of input energy of inelastic system is dissipated by the structural damping (the other part of input energy is dissipated by the inelastic deformation). The response reduction of elastic structure is larger than that of inelastic structure when the structural damping increases. Thus, in order to achieve the same target ductility, the strength reduction factor R_μ should decrease as the structural damping increases (Riddell and Newmark 1979a).

The most values of mean normalized R_μ in Fig. 12a are smaller than 1.2, and the most values of mean normalized R_μ in Fig. 12b are >0.9. Thus take the R_{DI} of $\zeta = 0.05$ as the benchmark, the influence of damping is commonly within 20 and 10 % for $\zeta = 0.02$ and 0.1 respectively.

5 Predictive model

The predictive model of the R_μ is an appealing tool to determine the R_μ in the seismic design. Based on the statistical results in Sect. 4 and boundary conditions of R_μ confirmed by many researchers which will be discussed in the following paragraphs, the predictive model is proposed as:

$$R_\mu = \frac{[a \cdot (\mu - 1) + 1] \cdot T^2 + b \cdot T^{0.5}}{T^2 + b \cdot T^{0.5}} \tag{4}$$

where, T is the period, μ is the ductility factor, a and b are regression parameters depending on the site classes, hysteretic models and relative peak ground acceleration of aftershock ground motion ∇PGA. The data of the statistical mean R_μ is used for the regression analysis. Parameters a and b are calculated by a nonlinear least-square regression analysis with the Levenberg–Marquardt method (Levenberg 1944; Marquardt 1963) for each site class, each hysteretic model and each ∇PGA. Table 4 summarizes resulting values of these regression parameters.

It should be noted that the derivation of the predictive model was heavily guided by the characteristics of R_μ and inspection of the data. The basic mathematical form of the

Table 4 The regression parameters of Eq. (4) for relative intensity being 0.0 (i.e. mainshock), 0.5, 0.8, 1.0 and 1.5

Hysteretic models	Site classes	*a*					*b*				
		0.0	0.5	0.8	1.0	1.5	0.0	0.5	0.8	1.0	1.5
EPP	A	1.29	1.24	1.17	1.13	1.05	0.30	0.29	0.30	0.31	0.40
	B	1.23	1.18	1.15	1.13	1.09	0.28	0.26	0.29	0.33	0.50
	C	1.37	1.12	1.35	1.34	1.30	0.64	0.14	0.67	0.73	0.86
	D	1.25	1.10	1.04	1.01	0.95	0.36	0.27	0.34	0.44	0.81
	All	1.28	1.18	1.17	1.14	1.09	0.36	0.29	0.37	0.41	0.59
MC	A	1.36	1.32	1.23	1.19	1.11	0.36	0.34	0.31	0.32	0.38
	B	1.38	1.36	1.34	1.32	1.30	0.29	0.29	0.31	0.36	0.54
	C	1.53	1.53	1.53	1.54	1.57	0.72	0.72	0.76	0.82	1.07
	D	1.49	1.36	1.26	1.22	1.17	0.43	0.37	0.43	0.54	0.98
	All	1.43	1.38	1.33	1.30	1.27	0.41	0.39	0.42	0.47	0.68
PH	A	1.29	1.26	1.17	1.13	1.05	0.45	0.46	0.41	0.43	0.49
	B	1.33	1.32	1.31	1.29	1.27	0.42	0.42	0.46	0.51	0.71
	C	1.52	1.52	1.53	1.54	1.55	1.13	1.13	1.19	1.25	1.47
	D	1.50	1.38	1.30	1.27	1.25	0.76	0.71	0.86	1.05	1.69
	All	1.39	1.36	1.31	1.29	1.25	0.63	0.62	0.66	0.73	0.97
SSD	A	1.41	1.37	1.27	1.23	1.15	0.50	0.48	0.44	0.45	0.51
	B	1.40	1.39	1.37	1.36	1.34	0.37	0.37	0.41	0.47	0.67
	C	1.59	1.60	1.60	1.63	1.63	0.95	0.96	1.00	1.12	1.31
	D	1.57	1.44	1.35	1.32	1.29	0.63	0.59	0.74	0.93	1.55
	All	1.48	1.43	1.38	1.36	1.33	0.57	0.55	0.60	0.68	0.91

predictive model is firstly developed based on the boundary conditions of R_μ, as explained in the next paragraph. Then the tentative exponents of T in the first and second terms of numerator and denominator are included in the initial form and the nonlinear least-square regression analysis is performed. These tentative exponents are adjusted based on the residuals, until the predictive model can give the good estimation of mean R_μ for different cases. With this procedure, the predictive model can be obtained with the good regression fit and fewer regression parameters.

The Eq. (4) rigorously satisfies the following boundary conditions:

$$R_\mu(T \to 0, \mu) = 1 \tag{5}$$

$$R_\mu(T, \mu = 1) = 1 \tag{6}$$

Many researches (Veletsos and Newmark 1960; Newmark and Hall 1969; Riddell and Newmark 1979a; Miranda 1993; Miranda and Bertero 1994) suggested that the R_μ of the extreme flexible structure tends to be the value of target ductility factor, because the maximum relative displacement tends towards the maximum ground displacement. This condition is not rigorously satisfied by the Eq. (4). However, for the long periods investigated in this manuscript, the predicted R_μ of Eq. (4) tends to be close to the target ductility factor and the differences are generally within 10 %.

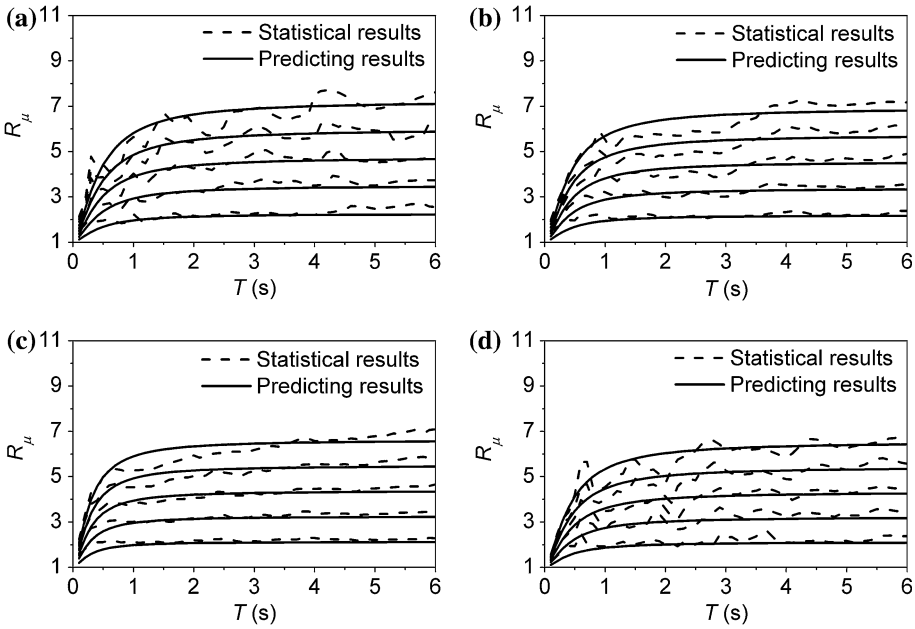

Fig. 13 The comparison of predicted mean R_μ using Eq. (4) with the statistical results for EPP system and sequence-type ground motion with $\nabla PGA = 0.5$: **a** site class A, **b** site class B, **c** site class C, **d** site class D

Figure 13 illustrates the comparison of predicted mean R_μ using Eq. (4) with the statistical results for EPP system and sequence-type ground motion with $\nabla PGA = 0.5$. It can be concluded that the Eq. (4) provide the good estimation of the mean R_μ.

It is important to compare the prediction results of Eq. (4) with the actual R_μ dataset of selected sequence-type ground motions. Based on the definition of FEMA 440 (2005), the following two error measures (i.e. sample mean error $E_{T,\mu}$ and the standard deviation of the error $\sigma_{T,\mu}$) are used to evaluate the accuracy of the Eq. (4).

$$E_{T,\mu} = \frac{1}{n}\sum_{i=1}^{n}\left[\frac{\tilde{R}_{T,\mu}}{(R_{T,\mu})_i}\right] \tag{7}$$

$$\sigma_{T,\mu} = \sqrt{\frac{1}{n-1}\sum_{i=1}^{n}\left[\frac{\tilde{R}_{T,\mu}}{(R_{T,\mu})_i} - E_{T,\mu}\right]^2} \tag{8}$$

where, n is the number of the ground motions, $(R_{T,\mu})_i$ is the result of ith ground motion computed by the nonlinear response history analysis, $\tilde{R}_{T,\mu}$ is the result predicted by the Eq. (4). The $E_{T,\mu}$ can provide the average bias of Eq. (4) and the$\sigma_{T,\mu}$ can provide the measure of the dispersion of the errors, when the Eq. (4) is used to estimate the R_μ. Figure 14 presents the error measures of Eq. (4) for the EPP system under sequence-type ground motions with $\nabla PGA = 0.5$ on all site classes. It can be seen that the Eq. (4) tend to underestimate the actual R_μ in the short period region at a level of <20 %, thus the Eq. (4) provides the conservative predicting results in short period region. In the medium-long period, the average error of Eq. (4) is generally within 10 %. In general, $\sigma_{T,\mu}$ has strong

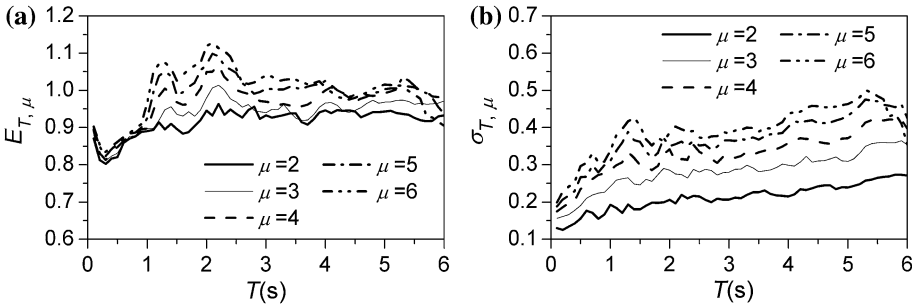

Fig. 14 The error measures of Eq. (4) for the EPP system under sequence-type ground motions with $\nabla PGA = 0.5$ on all site classes

dependence on the μ and increases with the increase of μ, meaning that the greater dispersion error would be induced when Eq. (4) is used to estimate the R_μ of greater μ.

In the seismic design practice, the relative intensity of aftershock ground motion in the given seismic zone should be determined through the seismic hazard analysis (i.e. to determine the hazard level of aftershock in the given seismic zone).

6 Conclusions

The purpose of this investigation is to propose the ductility-based strength reduction factor R_μ for the mainshock–aftershock sequence-type ground motions. The R_μ is computed with 458 sequence-type ground motions and four hysteretic models. The aftershock ground motions are scaled to have different relative intensity levels. The effect of aftershock on the R_μ is specially studied. The following conclusions are drawn from this investigation:

1. The R_μ in short period region is strongly dependent on the period, while that in medium-long period is approximately period independent. In the whole period region, mean R_μ increases with the increase of ductility factor μ. The influence of μ on the R_μ in short period region reduces gradually as the period decreases. The COV is approximately period independent.
2. The site condition has more obvious effect on the R_μ in short period region in comparison with the medium-long period region. In short period region, the mean R_μ on all site classes would overestimate the mean R_μ on site class D at a maximum level of 30 %, while mean R_μ on all site classes would underestimate the mean R_μ on site class A at a maximum level of 30 %.
3. The effect of aftershock ground motion with$\nabla PGA = 0.5$ on the R_μ of EPP system is negligible. The aftershock ground motion has similar effects on the R_μ for different hysteretic models. The aftershock ground motion with $\nabla PGA = 1.5$ can decrease the R_μ of structure with short period at a level of more than 20 %. The effects of aftershock on the COV of the R_μ can exceed 20 %. The influences of aftershock on the R_μ (mean and dispersion) depend on the period of structure, ductility factor and intensity of the aftershock ground motion.
4. The degrading behavior would decrease the R_μ of structure with short period at a magnitude of <20 %, while it would increase the R_μ of structure with medium-long period at a maximum level of 20 %. The R_μ decrease as the structural damping

increases and the effect level of damping on R_μ decreases as the structural damping increases.

5. The predictive model of the R_μ is proposed as a function of period, ductility factor. The regression parameters are dependent on the site classes, hysteretic models and relative intensity of aftershock ground motion ∇PGA. The predictive model can provide the good estimation of R_μ.

Acknowledgments This investigation is supported by the National Natural Science Foundation of China (Nos. 51322801,51238012 and 91215301), the Program for International Science and Technology Cooperation Projects of China (No. 2012DFA70810), the Program for New Century Excellent Talents in University of Ministry of Education of China (No. NCET-11-08), as well as the National Science and Technology Major Project (2013zx06002001-09). These supports are greatly appreciated. The authors are grateful to the anonymous reviewers for their constructive comments and suggestions.

References

Amadio C, Fragiacomo M, Rajgelj S (2003) The effects of repeated earthquake ground motions on the non-linear response of SDOF systems. Earthq Eng Struct Dyn 32:291–308

Augenti N, Parisi F (2010) Learning from construction failures due to the 2009 L'Aquila, Italy, earthquake. J Perform Constr Facil 24:536–555

Ceci AM, Contento A, Fanale L, Galeota D, Gattulli V, Lepidi M, Potenza F (2010) Structural performance of the historic and modern buildings of the University of L'Aquila during the seismic events of April 2009. Eng Struct 32:1899–1924

CEN (2003) Eurocode 8: Design of structures for earthquake resistance, part 1: general rules, seismic actions and rules for buildings. European Committee for Standardization, Brussels

Chakraborti A, Gupta VK (2005) Scaling of strength reduction factors for degrading elasto-plastic oscillators. Earthq Eng Struct Dyn 34:189–206

Das S, Gupta VK, Srimahavishnu V (2007) Damage-based design with no repairs for multiple events and its sensitivity to seismicity model. Earthq Eng Struct Dyn 36:307–325

Di Sarno L (2013) Effects of multiple earthquakes on inelastic structural response. Eng Struct 54:673–681

Efraimiadou S, Hatzigeorgiou GD, Beskos DE (2013) Structural pounding between adjacent buildings subjected to strong ground motions. Part II: the effect of multiple earthquakes. Earthq Eng Struct Dyn 42:1529–1545

Elnashai AS, Jefferson T, Fiedrich F, Cleveland LJ, Gress T (2009) Impact of New Madrid seismic zone earthquakes on the central USA: Volume I. Mid-America Earthquake (MAE) Center Repeort, No. 09-03

Faisal A, Majid TA, Hatzigeorgiou GD (2013) Investigation of story ductility demands of inelastic concrete frames subjected to repeated earthquakes. Soil Dyn Earthq Eng 44:42–53

FEMA 440 (2005) Improvement of nonlinear static seismic analysis procedures. June, chapter 3

Fragiacomo M, Amadio C, Macorini L (2004) Seismic response of steel frames under repeated earthquake ground motions. Eng Struct 26:2021–2035

Gillie JL, Rodriguez-Marek A, McDaniel C (2010) Strength reduction factors for near-fault forward-directivity ground motions. Eng Struct 32:273–285

Goda K (2012) Nonlinear response potential of mainshock–aftershock sequences from Japanese earthquakes. Bull Seismol Soc Am 102:2139–2156

Goda K, Taylor CA (2012) Effects of aftershocks on peak ductility demand due to strong ground motion records from shallow crustal earthquakes. Earthq Eng Struct Dyn 41:2311–2330

Han R, Li Y, van de Lindt J (2014) Seismic risk of base isolated non-ductile reinforced concrete buildings considering uncertainties and mainshock–aftershock sequences. Struct Saf 50:39–56

Hatzigeorgiou GD (2010a) Behavior factors for nonlinear structures subjected to multiple near-fault earthquakes. Comput Struct 88:309–321

Hatzigeorgiou GD (2010b) Ductility demand spectra for multiple near- and far-fault earthquakes. Soil Dyn Earthq Eng 30:170–183

Hatzigeorgiou GD (2010c) Ductility demands control under repeated earthquakes using appropriate force reduction factors. J Earthq Tsunami 4:231–250

Hatzigeorgiou GD, Beskos DE (2009) Inelastic displacement ratios for SDOF structures subjected to repeated earthquakes. Eng Struct 31:2744–2755
Hatzigeorgiou GD, Liolios AA (2010) Nonlinear behaviour of RC frames under repeated strong ground motions. Soil Dyn Earthq Eng 30:1010–1025
Iervolino I, Manfredi G, Cosenza E (2006) Ground motion duration effects on nonlinear seismic response. Earthq Eng Struct Dyn 35(1):21–38
International Building Code (IBC) (2006) International Code Council Inc., 4051 West Flossmoor Road, Country Club Hills
Jing LP, Liang HA, Li YQ, Liu CH (2011) Characteristics and factors that influenced damage to dams in the Ms 8.0 Wenchuan earthquake. Earthq Eng Eng Vib 10:349–358
Karakostas CZ, Athanassiadou CJ, Kappos AJ, Lekidis VA (2007) Site-dependent design spectra and strength modification factors, based on records from Greece. Soil Dyn Earthq Eng 27:1012–1027
Kunnath SK, Reinhorn AM, Park YJ (1990) Analytical modeling of inelastic seismic response of R/C structures. ASCE J Struct Eng 116(4):996–1017
Lee K, Foutch DA (2004) Performance evaluation of damaged steel frame buildings subjected to seismic loads. ASCE J Struct Eng 130:588–599
Levenberg K (1944) A method for the solution of certain non-linear problems in least squares. Q Appl Math 2:164–168
Li Q, Ellingwood BR (2007) Performance evaluation and damage assessment of steel frame buildings under mainshock–aftershock earthquake sequences. Earthq Eng Struct Dyn 36:405–427
Mahin SA, Bertero VV (1975) An evaluation of some methods for predicting seismic behavior of reinforced concrete buildings. Earthquake Engineering Research Center, University of California at Berkeley, CA; Report No. UCB/EERC-75/5
Mahin SA, Bertero VV (1976) Nonlinear seismic response of a coupled wall system. ASCE J Struct Eng 102:1759–1780
Marquardt D (1963) An algorithm for least-squares estimation of nonlinear parameters. SIAM J Appl Math 11:431–441
Miranda E (1993) Site-dependent strength-reduction factors. ASCE J Struct Eng 119:3503–3519
Miranda E, Bertero VV (1994) Evaluation of strength reduction factors for earthquake-resistant design. Earthq Spectra 10:357–379
Miranda E, Ruiz-García J (2002a) Influence of stiffness degradation on strength demands of structures built on soft soil sites. Eng Struct 24:1271–1281
Miranda E, Ruiz-García J (2002b) Evaluation of approximate methods to estimate maximum inelastic displacement demands. Earthq Eng Struct Dyn 31(3):539–560
Moustafa A, Takewaki I (2010) Modeling critical ground-motion sequences for inelastic structures. Adv Struct Eng 13:665–680
Newmark NM, Hall WJ (1969) Seismic design criteria for nuclear reactor facilities. In: Proceedings 4th World conference on earthquake engineering, Santiago, Chile, vol 4, pp 37–50
Palermo M, Silvestri S, Trombetti T, Landi L (2013) Force reduction factor for building structures equipped with added viscous dampers. Bull Earthq Eng 11:1661–1681
Qu H, Zhang J, Zhao JX (2011) Strength reduction factors for seismic analyses of buildings exposed to near-fault ground motions. Earthq Eng Eng Vib 10:195–209
Rahnama M, Krawinkler H (1993) Effects of soft soil and hysteresis model on seismic demands. John A. Blume Earthquake Engineering Center, chapter 3, pp 36–37
Riddell R, Newmark NM (1979a) Statistical Analysis of the response of nonlinear systems subjected to earthquakes. Structural Research Series No. 468, Department of Civil Engineering, University of Illinois
Riddell R, Newmark NM (1979b) Force-deformation models for nonlinear analyses. ASCE J Struct Div 105:2773–2778
Riddell R, Garcia JE, Garces E (2002) Inelastic deformation response of SDOF systems subjected to earthquakes. Earthq Eng Struct Dyn 31:515–538
Ruiz-García J (2012) Mainshock–aftershock ground motion features and their influence in building's seismic response. J Earthq Eng 16:719–737
Ruiz-García J, Negrete-Manriquez JC (2011) Evaluation of drift demands in existing steel frames under as-recorded far-field and near-fault mainshock–aftershock seismic sequences. Eng Struct 33:621–634
Ruiz-García J, Terán-Gilmore A, Díaz G (2012) Response of essential facilities under narrow-band mainshock–aftershock seismic sequences. In: Proceedings of the 15th World conference on earthquake engineering, Lisboa, Portugal. Paper 5382
Ruiz-García J, Marín MV, Terán-Gilmore A (2014) Effect of seismic sequences in reinforced concrete frame buildings located in soft-soil sites. Soil Dyn Earthq Eng 63:56–68

Sunasaka Y, Kiremidjian AS, Toki K (2002) Strength demand spectra with uniform damage level in lifetime of structure. ASCE J Struct Eng 48A:523–530

Tong G, Zhao Y (2007) Seismic force modification factors for modified-Clough hysteretic model. Eng Struct 29(11):3053–3070

Valles RE, Reinhorn AM, Kunnath SK, Madan A (1996) IDARC2D, version 4.0: a computer program for the inelastic damage analysis of buildings. National Center for Earthquake Engineering Research, State University of New York, Buffalo

Veletsos AS, Newmark M (1960) Effect of inelastic behavior on the response of simple systems to earthquake motions. In: Proceedings of the 2nd World conference on earthquake engineering, Tokyo, Japan, pp 895–912

Wen WP, Zhai CH, Li S, Chang Z, Xie LL (2014) Constant damage inelastic displacement ratios for the near-fault pulse-like ground motions. Eng Struct 59:599–607

Zhai CH, Wen WP, Chen Z, Li S, Xie LL (2013a) Damage spectra for the mainshock–aftershock sequence-type ground motions. Soil Dyn Earthq Eng 45:1–12

Zhai CH, Wen WP, Zhu TT, Li S, Xie LL (2013b) Inelastic displacement ratios for design of structures with constant damage performance. Eng Struct 52:53–63

Zhai CH, Wen WP, Li S, Chen Z, Chang Z, Xie LL (2014) The damage investigation of inelastic SDOF structure under the mainshock–aftershock sequence-type ground motions. Soil Dyn Earthq Eng 59:30–41

Zhang S, Wang G, Sa W (2013) Damage evaluation of concrete gravity dams under mainshock–aftershock seismic sequences. Soil Dyn Earthq Eng 50:16–27